Dynamic Contrast-enhanced Magnetic Resonance Imaging as a Predictor of Clinical Outcome in Canine Spontaneous Soft Tissue Sarcomas Treated with Thermoradiotherapy

Benjamin L. Viglianti,[1] Michael Lora-Michiels,[1] Jeanie M. Poulson,[1] Lan Lan,[2] Dahio Yu,[5] Linda Sanders,[2] Oana Craciunescu,[1] Zeljko Vujaskovic,[1] Donald E. Thrall,[4] James MacFall,[3] Cecil H. Charles,[3] Terence Wong,[3] and Mark W. Dewhirst[1]

Abstract

Purpose: This study tests whether dynamic contrast-enhanced magnetic resonance imaging (DCE-MRI) parameters obtained from canine patients with soft tissue sarcomas, treated with hyperthermia and radiotherapy, are predictive of therapeutic outcome.

Experimental Design: Thirty-seven dogs with soft tissue sarcomas had DCE-MRI done before and following the first hyperthermia. Signal enhancement for tumor and reference muscle were fitted empirically, yielding a washin/washout rate for the contrast agent and tumor area under the signal enhancement curve (AUC) calculated from 0 to 60 seconds, 90 seconds, and the time of maximal enhancement in the reference muscle. These parameters were then compared with local tumor control, metastasis-free survival, and overall survival.

Results: Pretherapy rate of contrast agent washout was positively predictive of improved overall and metastasis-free survival with hazard ratio of 0.67 ($P = 0.015$) and 0.68 ($P = 0.012$), respectively. After the first hyperthermia washin rate, AUC60, AUC90, and AUCt-max were predictive of improved overall and metastasis-free survival with hazard ratio ranging from 0.46 to 0.53 ($P < 0.002$) and 0.44 to 0.55 ($P < 0.004$), respectively. DCE-MRI parameters were compared with extracellular pH and ^{31}P MR spectroscopy results (previously published) in the same patients showing a correlation. This suggested that an increase in perfusion after therapy was effective in eliminating excess acid from the tumor.

Conclusions: This study shows that DCE-MRI has utility predicting overall and metastasis-free survival in canine patients with soft tissue sarcomas. To our knowledge, this is the first time that DCE-MRI parameters are predictive of clinical outcome for soft tissue sarcomas.

Numerous phase III clinical trials have shown that thermoradiotherapy is superior to radiotherapy alone for achieving local tumor control and, in some cases, improving survival (1–6). It is well known that hyperthermia changes tumor oxygenation, inhibits DNA damage repair, and is directly cytotoxic (7, 8). The effects described above are strongly dependent on temperature and duration of heat exposure, but which effect dominates in improving tumor control with thermoradiotherapy is not known. In preclinical models, mild to moderate heating (41-43°C) leads to increased perfusion and oxygenation, whereas higher thermal exposures can cause vascular damage and hypoxia (8). Presumably, this latter effect would be deleterious to optimal thermoradiotherapy response, but there are no definitive clinical studies showing this.

Previous work with canine sarcomas have reported improved oxygenation following a single hyperthermia treatment when median temperatures were <44°C (9) and that changes in oxygenation can persist throughout a course of fractionated thermoradiotherapy (10). Milligan and Panjehpour (11) reported that perfusion was improved throughout a course of thermoradiotherapy in dogs with mast cell tumors. These data support the notion that part of the effect that mild hyperthermia has in improving radiotherapy response is due to increased oxygenation through improved perfusion. However, in neither of these reports was there a correlation made between changes in pO_2 or perfusion and treatment outcome.

Brizel et al. (12) reported that improvements in oxygenation 24 hours after the first hyperthermia treatment were associated with higher pathologic complete response rates after

Authors' Affiliations: Departments of [1]Radiation Oncology, [2]Biostatistics and Bioinformatics, and [3]Radiology, Duke University Medical Center, Durham, North Carolina, [4]School of Veterinary Medicine, North Carolina State University, Raleigh, North Carolina, and [5]Department of Biostatistics, Oncologic Sciences, Moffit Cancer Center and Research Institute, Tampa Florida

Received 9/9/08; revised 3/16/09; accepted 4/6/09; published OnlineFirst 7/21/09.

Grant support: NIH grant PO1CA42745 from the Department of Health and Human Services.

The costs of publication of this article were defrayed in part by the payment of page charges. This article must therefore be hereby marked *advertisement* in accordance with 18 U.S.C. Section 1734 solely to indicate this fact.

Note: Supplementary data for this article are available at Clinical Cancer Research Online (http://clincancerres.aacrjournals.org/).

B.L. Viglianti and M. Lora-Michiels contributed equally to this work.

Current address for M. Lora-Michiels: School of Veterinary Medicine, Tufts University, North Grafton, MA 01536. Current address for J.M. Poulson: School of Veterinary Medicine, Purdue University, West Lafayette, IN 47907.

Requests for reprints: Mark W. Dewhirst, Department of Radiation Oncology, Duke University Medical Center, Box 3455, Durham, NC 27710. Phone: 919-684-4180; Fax: 919-684-8718; E-mail: dewhi001@mc.duke.edu.

doi:10.1158/1078-0432.CCR-08-2222

Translational Relevance

This study shows the ability to predict overall and metastasis-free survival of canine patients with soft tissue sarcomas using magnetic resonance imaging (MRI) before and 24 hours after the neoadjuvant hyperthermia/radiation therapy. In soft tissue sarcomas, early metastasis is a common problem, requiring aggressive neoadjuvant, surgery, and adjuvant therapy to have a favorable outcome. The ability to use dynamic contrast-enhanced MRI to stratify these patients would have significant clinical effect in its subsequent potential to influence the aggressiveness of neo/adjuvant therapy along with determining if the therapy will be an effective treatment. To our knowledge, this is the first study to show the use of dynamic contrast-enhanced MRI in soft tissue sarcomas and have an independent predictive ability on treatment efficacy.

thermoradiotherapy of human soft tissue sarcomas. Jones et al. (13) presented similar data in a small series of 13 patients with locally advanced breast cancer who were treated with a combination of hyperthermia, paclitaxel, and radiotherapy. The response end points reported in both of these studies were relevant to short-term cell killing, but neither addressed the more important issue of the effects of reoxygenation on local tumor control.

Because of the importance of perfusion in cancer therapy (with or without hyperthermia), dynamic contrast-enhanced magnetic resonance imaging (DCE-MRI) has been gaining use to obtain physiologic information. This imaging method provides information related to perfusion and permeability-surface to volume product of a region/voxel of interest.

Recently, we reported results from a randomized phase II clinical trial involving thermoradiotherapy treatment of canine soft tissue sarcomas (3). Results of this trial indicated that higher thermal dose was associated with significant prolongation of progression-free survival. Extracellular pH (pHe) and ^{31}P MR spectroscopy parameters were associated with metastasis-free and overall survival in a subset of patients from this same trial (14). In this particular study, we evaluate the potential of DCE-MRI–derived parameters, obtained before treatment and 24 to 72 hours after first hyperthermia treatment, to be prognostically predictive in subset of 37 patients who were evaluated with MRI as part of this trial.

Materials and Methods

Patients and clinical trial design. Thirty-seven canine patients with spontaneously occurring soft tissue sarcomas were randomized to receive either a low (2-5) or high (20-50) thermal dose quantified as cumulative equivalent minutes that the T90 was equal to 43°C (CEM43°C T90), in combination with fractionated radiotherapy (56.25 Gy in 25 daily fractions of 2.25 Gy). T90 refers to the temperature reached or exceeded by 90% of measured temperature points. Tumor types included 20 hemangiopericytomas (54.1%), 9 fibrosarcomas (24.3%), 4 myxosarcomas (10.8%), 2 neurofibrosarcomas (5.4%), and 2 nonspecific sarcomas (5.4%). Classification of histologic subtype was done by a board-certified veterinary pathologist (15). Hyperthermia was induced using microwave applicators operating between 140 and 433 MHz. Thermal dose randomization was stratified by tumor volume and tumor grade. Approximately one hyperthermia treatment was given per week, after the daily radiation fraction. The duration of the hyperthermia treatment was adjusted so as to administer ~20% of the prescribed hyperthermia total dose in each hyperthermia fraction. Occasionally, the prescribed thermal dose was administered in 4 weekly treatments, and in some other dogs, a sixth treatment had to be added to reach the prescribed thermal dose (3). MRI was done before and 24 to 72 h after the first hyperthermia treatment (Fig. 1).

The procedures were approved by the North Carolina State and Duke University Animal Care and Use Committees.

DCE-MRI acquisition. All studies were done on a GE 1.5T Signa System equipped with a surface coil. Dogs were anesthetized with isoflurane (Abbott Laboratories) for the MR study. Coronal and axial localizer images (fast spoiled gradient recalled echo pulse sequence) were acquired initially to define tumor position. Five baseline scans consisting of 15 T1-weighted images (repetition time = 400; echo time = 15) per volume were acquired before contrast injection (field of view = 256 × 128; slice thickness = 5-10 mm). Subsequently, an i.v. bolus injection (0.1 mmol/kg, 2 mL/s) of gadolinium dimeglumine (Gd-DTPA) was administered. Image volumes were acquired every 30 s for 20 min.

Image analysis. Relative enhancement images were fitted pixel by pixel with a double exponential Eq. A using a nonlinear iterative χ^2 minimization technique based on the marquadt algorithm.

$$\Delta\text{Signal} = \text{Smax} * (1 - \exp(-\text{alpha} * \text{time})) * \exp(-\text{beta} * \text{time}) \quad \text{(A)}$$

Each fitted curve allowed the extraction of Smax (relative maximal enhancement constant), alpha (delivery rate constant), and beta (clearance rate constant) parameters. Negative values or values from the fit that never converged were not included for calculations of region of interest analysis. These parameters allowed the calculations of washin rate (Smax * α) and washout rate (Smax * β) along with area under the signal enhancement curve (AUC). With these parameters, descriptors of perfusion/permeability were obtained (16, 17). For evaluation of AUC, three different integration times were chosen for calculation, AUC60 (integration time from 0 to 60 s), AUC90 (integration time from 0 to 90 s), and AUCt-max (integration time from 0 to when the muscle reference signaled peaked, t-max). Time to maximal muscle enhancement was calculated by setting the derivative of Eq. A to zero and solving for time. Otherwise, this last value was used as the upper limit for calculating AUCt-max. Representative patient image data are shown in Fig. 2 for pre- and post-hyperthermia images and pseudo-false color for washin, washout, and AUCt-max data.

From the fitted data, region of interest for tumor (including any necrosis) and muscle was manually drawn on each slice to form volumes of interest. Tumor region of interest included the entire tumor and potential necrosis, and the muscle region of interest was drawn on muscle free of tumor in the field of view based on known normal anatomy. Median values were extracted from each volume of interest. Washin, washout, AUC60, AUC90, and AUCt-max parameters were analyzed individually. This yielded five different parameters relating to perfusion/permeability. All imaging analyses were made with a custom-made software running on MATLAB (The MathWorks, Inc.).

pH measurements. pHe measurements were made using needle microelectrodes (Microelectrode, Inc. and Agulian), as previously described. Multiple measurements were made and averaged to obtain an overall estimate of the pHe. Intracellular pH (pHi) was determined by the frequency difference between the Pi and PCr resonances, from ^{31}P MR spectroscopy spectra. MR spectroscopy spectra were acquired with a surface dual frequency coil array, and triphenyl phosphite standard solutions were placed next to the tumor for pulse calibration. Pulse sequence protocol and data analysis methods have been previously reported in detail (2, 14, 18).

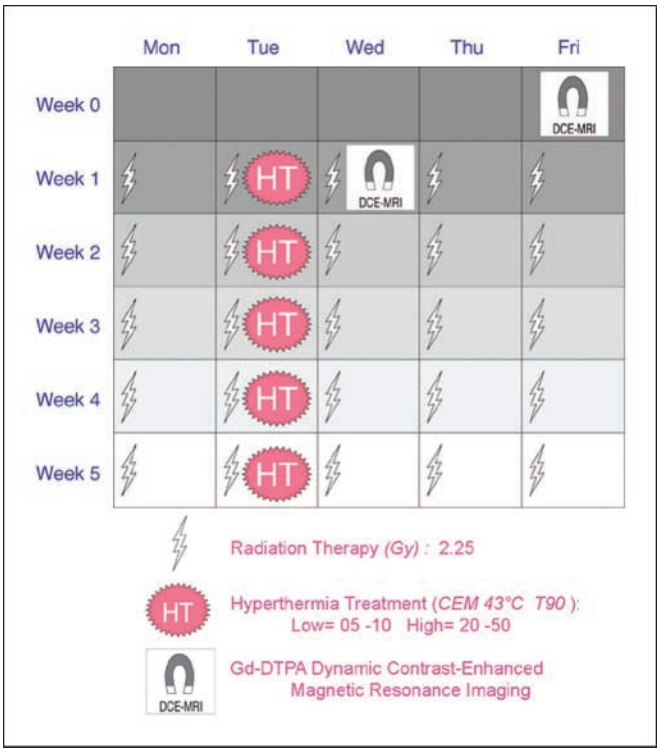

Fig. 1. Graphical representation of the treatment and MRI acquisition schedule for this trial.

Treatment end points. After treatment, dogs were reevaluated at 1, 2, 3, 5, 7, 9, and 12 mo and then at 3-mo intervals. Reevaluation consisted of physical examination, tumor measurement, thoracic radiographs, and assessment of regional lymph nodes. Tumors volumes were determined by direct physical measurements along 3 axis multiplied together with PI/6. Duration of local tumor control was defined as the time from date of the first hyperthermia treatment until local failure. Metastasis-free survival was defined as the time from date of the first hyperthermia treatment until metastasis or death, and overall survival was the time from date of the first hyperthermia treatment until death from any cause. Spread to regional lymph nodes was classified as positive for metastasis, as well as any spread to distant organs, such as the lung.

Statistical analysis. Values of AUC were log transformed due to the large range of calculated values; therefore, throughout the article, AUC values reported will correspond to $\log_{10}$(AUC) values.

Each perfusion parameter was assessed for its predictive properties on metastasis-free survival, time to local failure, and overall survival, before and after treatment, as well as their difference post-pre (Δ) treatment, using Cox proportional hazard ratio and log-rank tests. The effect of the first hyperthermia treatment, as described by T50, T90, CEM43°C T50, and CEM43°C T90, along with administration time of hyperthermia on perfusion parameters obtained after the first hyperthermia, was assessed using a Wilcoxon rank sum test as well as a paired *t* test.

With one exception, multiregression was not attempted for correlation with treatment outcome because of the limited number of subjects. Univariable and multivariable analyses were done between perfusion-related parameters and other clinical variables as well as the pH parameters to determine whether these were related to each other. Corrections for multiple comparisons were not made.

Results

Thirty-seven dogs (median age = 9.8 years; interquartile range = 4.3 years) were evaluated with DCE-MRI before starting treatment. Seventeen of the dogs had a second DCE-MRI 24 hours after the first thermoradiotherapy treatment. All subjects were planned to receive the second DCE-MRI study, but in 20 of these subjects, the data were not obtained either because of scheduling issues or because clean spectroscopic data could not be derived from the tissue for the second session, which was required before the DCE-MRI per protocol design. The descriptive statistics of the sample characteristics are listed by thermal dose group in Table 1.

Thermal parameters

The population was balanced with respect to thermal dose group (low dose = 56.7%; high dose = 43.3%). In the high thermal dose group, median temperature averaged T50 (median = 43.2°C; interquartile range = 1.9°C), T90 (median = 40.8°C; interquartile range = 0.7°C), CEM43°C T50 (median = 89.1 minutes; interquartile range = 144.8 minutes), and CEM43°C T90 (median = 8.2 minutes; interquartile range = 6.4 minutes) and the total duration time of heating (median = 214 minutes; interquartile range = 179.5 minutes). In the low thermal dose group, median temperature averaged T50 (median = 42.6°C; interquartile range =1.7°C), T90 (median = 39.9°C; interquartile range = 0.6°C), CEM43°C T50 (median = 17.5 minutes; interquartile range = 32.0 minutes), and CEM43°C T90 (median = 0.8 minute; interquartile range = 0.6 minute)

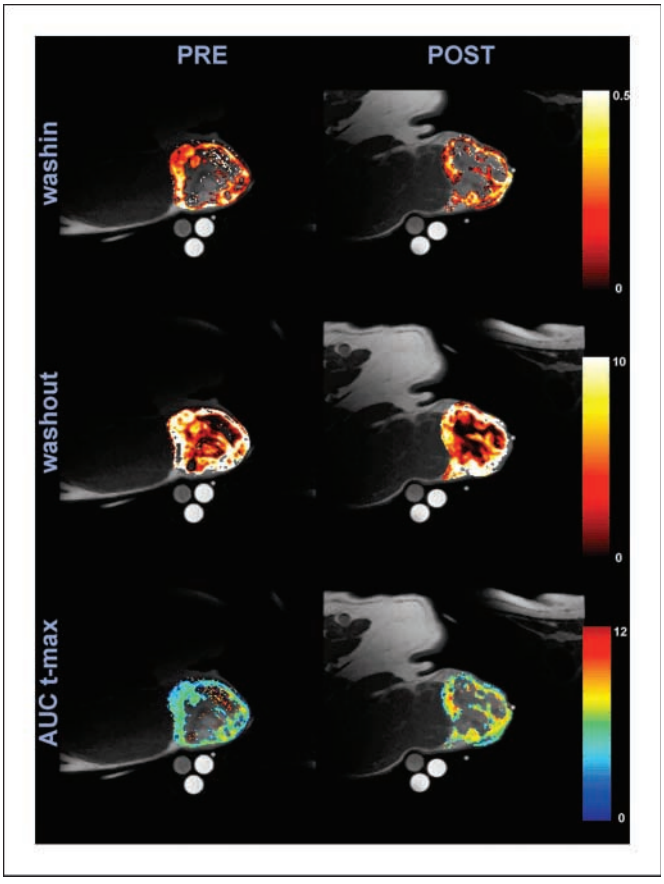

Fig. 2. Overlay of anatomic T1 images with washin, washout, and AUCt-max perfusion maps obtained from a canine patient with a hemangiopercytoma of the perineum using DCE-MRI. Note the heterogeneity in tumor perfusion and the increase in AUCt-max after 24-h post-hyperthermia. AUCt-max is the AUC of the dynamic signal enhancement between 0 and the time of maximal muscle enhancement. AUC values are expressed in $\log_{10}$.

Table 1. Sample characteristics by thermal dose group

Variable	Low dose, mean (SD) or % (n = 21)	High dose, mean (SD) or % (n = 16)	All subjects, mean (SD) or % (n = 37)
Age (y)	10.1 (2.8)	10.1 (3.1)	10.1 (2.9)
Tumor volume (cm^3)	48.6 (69.0)	44.5 (42.2)	46.8 (58.2)
Low tumor grade	76.2%	62.5%	70.3%
High tumor grade	23.8%	37.5%	29.7%
FSA histology type	14.3%	25%	18.9%
HPC histology type	52.4%	50%	51.4%
MYX histology type	9.5%	12.5%	10.8%
NFS histology type	4.8%	6.3%	5.4%
SA histology type	9.5%	0	5.4%
Other histology type	9.5%	6.2%	8.1%

NOTE: Descriptive statistics of the treated tumors separated by thermal dose groups. Histologic types are expressed as a percentage of the total population.
Abbreviations: FSA, fibrosarcoma; HPC, hemangiopericytoma; MYX, myxosarcoma; NFS, neurofibrosarcoma; SA, sarcoma.

and the total duration time of heating (median = 103 minutes; interquartile range = 58 minutes).

The T50 and T90 values are descriptions of the frequency distribution of temperatures that are measured during treatment. The T50 is the median temperature and the T90 describes the temperature value that is exceeded by 90% of the measured values. This is sometimes referred to as the 10th percentile, but in the hyperthermia literature, it has been traditionally referred to as the T90. CEM43 °C is a conversion algorithm that converts any time-temperature history into an equivalent number of minutes at 43°C. Details of this algorithm are published elsewhere (19).

Predictors of clinical outcome

Cox proportional hazard ratio analyses showed that several imaging-based parameters obtained before and after the first hyperthermia treatment were found to be significant in predicting metastasis-free survival, time to local failure, and overall survival along with total duration of heating (Table 2).

Local tumor control. AUCt-max (median = 5.1; interquartile range = 0.65) measured before therapy was predictive of time to local failure (P = 0.02; Fig. 3A). There was no significant correlation between AUCt-max and tumor volume or grade in univariable analysis (Table 3). However, because of competing risks of animals developing distant disease before reaching an end point for local tumor control, caution needs to be considered with respect to how to interpret this result.

Metastasis-free and overall survival. The median time to metastasis was 24 months and the 2-year overall survival rate was 0.36. This included animals that died and at necroscopy metastasis were found. Pretreatment parameters that were found to be significant predictors of metastasis-free and overall survival included tumor grade ($P \leq 0.01$; 70%; intermediate/high = 30%), volume ($P < 0.05$; median = 18.8 cm^3; interquartile range = 55.7 cm^3), and washout ($P \leq 0.02$; median = 4.24; interquartile range = 2.72; shown in Fig. 3B). Better prognosis was associated with lower grade, smaller volume, and higher washout rate. The predictability of pHe parameters (obtained using microelectrodes) from Lora-Michiels et al. (14) is shown for comparison because these measurements were taken on the same subjects (Table 2).

AUCt-max, AUC60, AUC90, and washin parameter (Fig. 3C) obtained 24 hours following the first hyperthermia treatment were also significantly correlated with outcome. In all cases, higher values were associated with improved prognosis. These data suggest that improvements in perfusion and perhaps oxygenation after hyperthermia treatment are a good prognostic sign.

Multivariable analysis showed that pretreatment AUCt-max and washout were independent predictors of metastasis-free and overall survival ($P < 0.05$; Table 3). In contrast, univariable analysis showed that AUCt-max obtained after treatment was inversely related to tumor volume and tumor grade. Small and/or low-grade tumors had higher AUCt-max values ($P < 0.05$; Table 3). Washout and AUC values obtained after treatment also were negatively correlated with tumor volume in univariable analysis ($P < 0.05$; Table 3).

Duration of hyperthermia

The total duration of hyperthermia was found to be prognostically important in our previous report (3). In this subset analysis, duration of heating remained an independent predictor of metastasis-free and overall survival with hazard ratios of 1.28 and 1.32 and P values of 0.007 and 0.004, respectively (Table 2). In this current study, heating duration was correlated with tumor grade in a univariable analysis ($P < 0.05$; Table 3).

Relationship with pH

Relationships between the MRI parameters measured here and pH parameters reported in our previous article (14) are shown in Table 4. univariable analysis showed that post-hyperthermia washout values were negatively correlated with pretreatment pHi ($P < 0.05$; Table 4) and positively correlated with the difference posttreatment (post-pre) pHe ($P < 0.05$; Table 4). Figure 3D depicts the relationship of post-washout with the change of pHe showing a positive relationship, consistent with the notion that improved perfusion after heating leads to more efficient clearance of acid from the tissue.

Discussion

This study showed that DCE-MRI–based parameters may be useful in predicting overall and metastasis-free survival in canine patients with soft tissue sarcomas. The parameters from

the signal enhancement curve allowed prediction of patient outcome regardless of being done before the first hyperthermia therapy or 24 hours after. To our knowledge, this is the first time that DCE-MRI parameters are predictive of clinical outcome for patients with soft tissue sarcomas. However, the results are based on a few patients, so larger clinical trials with adequate statistical power are needed to verify this initial result.

Measurements taken before treatment

For data acquired before treatment, AUCt-max emerged as being related to local tumor control. This parameter integrates signal over time for the tumor, truncating it when the signal reaches a maximum value in the reference muscle tissue. Consequently, this parameter probably relates to both perfusion and permeability. Tumors with higher AUCt-max might be better perfused and therefore better oxygenated. In univariable analysis, this parameter was not associated with either tumor volume or grade, suggesting that it is an independent predictor of local tumor control (Table 3).

Higher washout values obtained before treatment were associated with greater metastasis-free and overall survival. This parameter relates to the reabsorption and clearance of contrast agent from the extravascular space. Thus, higher values maybe associated with a vasculature that is more efficient in transport. Factors that influence transport efficiency include vascular density, permeability, and perfusion rate of the microvessels (20–23).

In prior studies, we showed theoretically that adjustments in microvessel orientation can make quite dramatic differences in oxygen transport (20, 21). The same principle should apply in reverse for a MR contrast agent. Thus, the combination of vascular density and orientation of microvessels is likely to contribute significantly to the differences in washout between different tumors.

Vascular permeability is related to the size of the solute, the concentration gradient across the microvessel wall, and the physical characteristics of the vascular wall, due to the presence of large endothelial cell gaps and lack of basement membrane leading to increased permeability (24, 25). For large solutes, such as proteins, transport is strongly governed by convection generated by the pressure gradient across the vascular wall. With the presence of elevated tumor interstitial fluid pressure, these gradients are negligible (24, 25). However, small molecules also undergo diffusive transport, so the influence of convection on the transport of a small molecule such as a chelated Gd contrast agent is negligible. Consequently, the Gd would likely be reabsorbed into the vasculature down its own concentration gradient once the kidneys clear the Gd from the general circulation (24, 25).

It is difficult to know why animals with tumors with better transport characteristics would have longer metastasis-free and overall survival. It may be reflective of a more differentiated state, but washout was not significantly associated with either tumor size or grade, suggesting that it could be independently

Table 2. Statistical results, hazard analysis for metastasis-free survival, time to local failure, and overall survival

Parameter		MFS		TLF		OS	
	I.C	HR (95% CI)	*P*	HR (95% CI)	*P*	HR (95% CI)	*P*
Pre (n = 37)							
Grade	H vs L	**1.63 (1.1-2.4)**	**0.010**	1.36 (0.8-2.3)	0.230	**1.65 (1.1-2.4)**	**0.008**
Volume	27.9 cm^3	**1.15 (1.0-1.3)**	**0.049**	1.05 (0.8-1.3)	0.620	**1.16 (1.0-1.3)**	**0.040**
AUC60	0.3	0.80 (0.6-1.1)	0.220	0.88 (0.6-1.4)	0.582	0.81 (0.6-1.2)	0.247
AUC90	0.3	0.80 (0.6-1.1)	0.209	0.87 (0.6-1.4)	0.562	0.81 (0.6-1.1)	0.234
AUCt-max	0.3	0.89 (0.7-1.1)	0.310	**0.66 (0.5-0.9)**	**0.020**	0.89 (0.7-1.1)	0.320
Washin	0.1	0.89 (0.7-1.1)	0.331	0.86 (0.6-1.2)	0.381	0.89 (0.7-1.1)	0.338
Washout	1.4	**0.68 (0.5-0.9)**	**0.015**	0.87 (0.6-1.3)	0.500	**0.67 (0.5-0.9)**	**0.012**
Post (n = 17)							
AUC60	0.3	**0.44 (0.3-0.7)**	**0.001**	0.84 (0.5-1.5)	0.540	**0.49 (0.3-0.8)**	**0.001**
AUC90	0.3	**0.45 (0.3-0.7)**	**0.001**	0.85 (0.5-1.5)	0.550	**0.49 (0.3-0.8)**	**0.001**
AUCt-max	0.4	**0.46 (0.3-0.8)**	**0.002**	0.65 (0.4-1.2)	0.170	**0.46 (0.3-0.8)**	**0.001**
Washin	0.1	**0.55 (0.4-0.9)**	**0.004**	0.76 (0.5-1.3)	0.270	**0.53 (0.3-0.8)**	**0.002**
Washout	1.7	0.82 (0.5-1.3)	0.414	1.16 (0.6-2.1)	0.65	0.82 (0.5-1.3)	0.402
pH							
pHi-Pre (n = 30)	H vs L	0.54 (0.2-1.3)	0.150	0.49 (0.2-1.5)	0.199	0.58 (0.3-1.3)	0.199
pHi@24 h-pHi-Pre (n = 15)	H vs L	1.44 (0.5-4.6)	0.538	7.70 (0.9-66.2)	0.063	1.41 (0.4-4.5)	0.565
pHe-Pre (n = 30)	H vs L	**0.29 (0.1-0.7)**	**0.005**	0.84 (0.27-2.60)	0.767	**0.36 (0.2-0.8)**	**0.013**
pHe@24 h-pHe-Pre (n = 24)	H vs L	**2.87 (1.1-7.6)**	**0.034**	1.59 (0.5-5.5)	0.465	2.54 (1.0-6.7)	0.061
HTmin							
Total duration of heat (min)		**1.28 (1.1-1.5)**	**0.007**	1.18 (0.9-1.5)	0.149	**1.32 (1.09-1.60)**	**0.004**

NOTE: Summary of Cox proportional hazard ratio analysis showing significant perfusion/permeability predictors of clinical outcome determined with signal-based DCE-MRI. The pre-washout rate was predictive for metastasis-free and overall survival, whereas AUCt-max was predictive in time to local failure. For the post-image analysis, all the AUC calculation and the washin rates were predictive of metastasis-free and overall survival. The pre-pHe, the difference in pHe between pretherapy and posttherapy, and heating duration were also predictive of metastasis-free and overall survival.

Abbreviations: OS, overall survival; MFS, metastasis free survival; TLF, tumor local failure; I.C, incremental change (of respective unit); HR, hazard ratio; 95% CI, 95% confidence interval; AUC60, AUC integrated up to 60 s; AUC90, AUC integrated up to 90 s; AUCt-max, AUC integrated up to time to muscle peak.

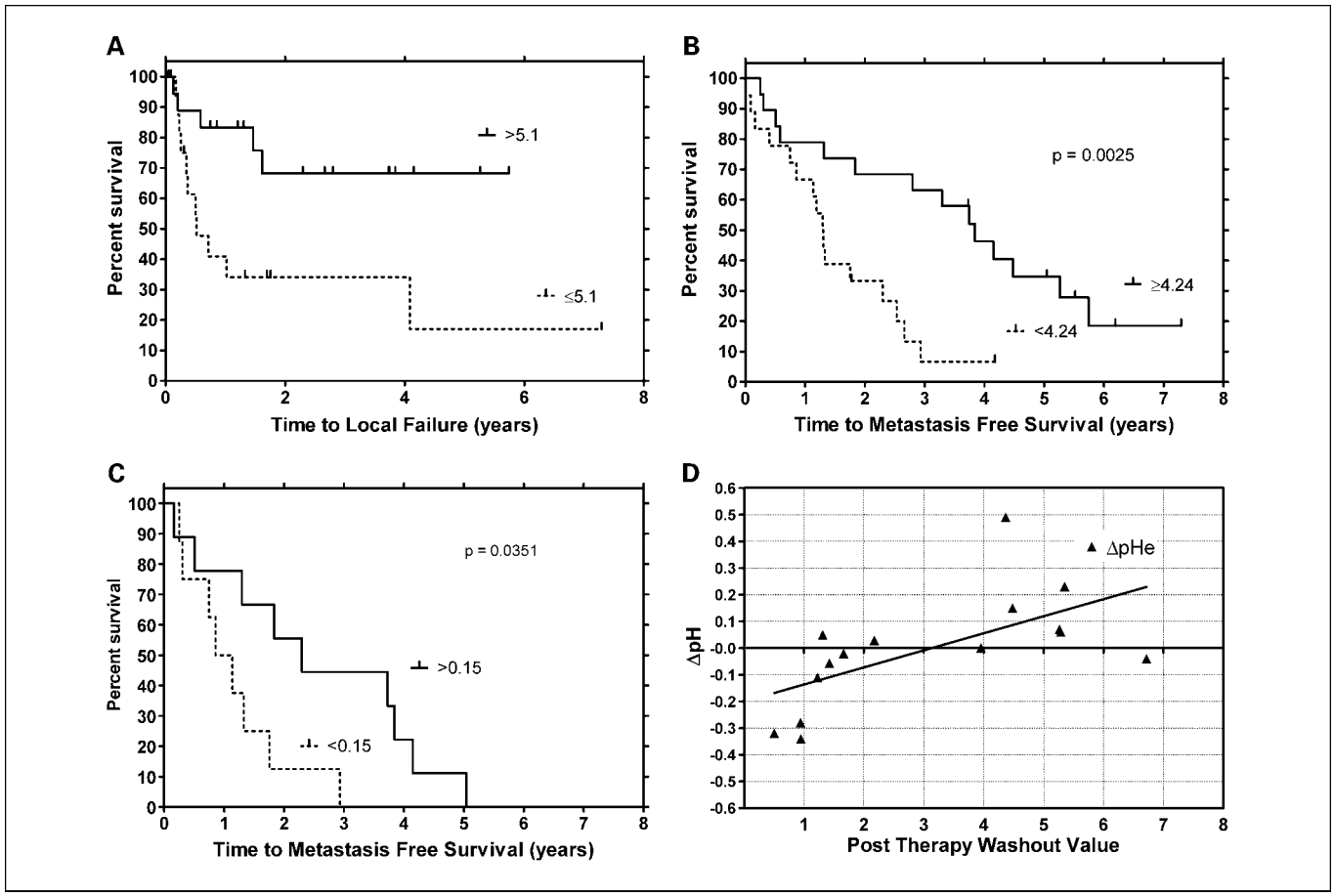

Fig. 3. *A,* Kaplan-Meier plot depicting time to local failure for tumors with AUCt-max values (expressed in $\log_{10}$ form) above and below their cut point values (cut point = interquartile range/2). Kaplan-Meier plot depicting metastasis-free survival for tumors with washout values above and below their cut point values (cut point = interquartile range/2) before treatment (*B*) and washin 24 h after hyperthermia with a similarly calculated cut point (*C*). *D,* relationship of pHi-Pre and pHe@24 h-pHe-Pre versus washout measured with DCE-MRI. pHi before therapy shows a negative correlation with increasing post-washout values. Changes in pHe from therapy show a positive correlation with increase post-washout values. This suggests that following therapy the ability to remove the contrast agent results is greater ability to also remove acid from the extracellular environment of tumors that are more acidic before therapy. This agrees with the assumption that hyperthermia improves perfusion and removal of the contrast agent is suggestive of this.

predictive of outcome (Table 3). Current studies by our group are investigating interrelationships between physiologic/metabolic and genomic parameters compared with DCE-MRI. From this, we may decipher more insight into this observation.

Measurements taken after the first heat treatment

It was surprising to find that DCE-MRI values obtained after the first hyperthermia treatment were also associated with outcome. Increases in AUC and washin after the first heat treatment were associated with prolonged metastasis-free and overall survival (Table 3). This may relate back to the maturity of the vasculature. AUCt-max values (along with other parameters) for the posttreatment study were correlated with tumor volume and grade, suggesting that they may not be independent predictors of outcome. It is known that hyperthermia causes changes in permeability/perfusion but the distribution and amount may be dependent on the tumor volume/aggressiveness. Tumors with more mature vasculature may be able to respond more dynamically to thermal stress and therefore more readily increase perfusion in response to thermal stress. Presumably, tumors with more mature vasculature might be less likely to metastasize for a variety of reasons. They may be less hypoxic, which would tend to reduce up-regulation of transcription factors that influence metastatic propensity, such as hypoxia inducible factor-1 (26).

DCE-MRI as a clinical predictor

Only a few studies have been published describing the prognostic properties of DCE-MRI for clinical efficacy; studies involving gliomas, head and neck, breast, lung, and cervical cancers have been reported (Supplementary Table S1). However, to our knowledge, clinical studies involving prediction of outcome for soft tissue sarcomas using DCE-MRI have not been reported.

AUCt-max was the only perfusion parameter to predict local failure in our study (Table 2). Similar results have been reported by Mayr et al. (27, 28) in patients with cervical carcinomas at early stages of radiation therapy using relative signal intensity parameters (Supplementary Table S1).

Two studies have evaluated DCE-MRI parameters after treatment. Decreased tumor perfusion, at the end of a course of fractionated radiotherapy assessed by signal intensity perfusion indexes (initial slope, T_{max}), was related to low rates of local recurrence in patients with head and neck cancer (29).

Decreased perfusion indexes using the two-compartment model, K^{trans} and V_e, had >65% tumor volume reduction after multimodality therapy in patients with breast cancer (30). Similar to the head and neck trial, these results are not surprising given they were obtained following therapy.

Although studies done at the end of primary therapy are of interest scientifically, as they suggest that therapy eventually leads to reduction in perfusion, such information would have little effect on therapeutic choices. A more desirable approach is to predict likelihood of local control before or during the early phases of treatment because such measurements could be used to alter the course of treatment and potentially lead to increased treatment efficacy.

Metastasis-free and overall survival

Our results show that longer metastasis-free survival and increased overall survival occurred in dogs with highly perfused tumors before hyperthermia treatment measured by increased washout rate and after treatment with increased washin rate, AUC60, AUC90, and AUCt-max. Only one other study has been published that relates to these end points. An increased incidence of metastasis (and poorer survival) was observed in patients with Ewing's sarcomas displaying high percentage of necrosis (31). The percentage of necrosis was obtained by calculating nonenhanced tumor regions from pre– and post–contrast-enhanced images. Although this study did not specifically use dynamic MR parameters, lack of contrast agent is due to a lack of delivery (i.e., perfusion).

Thermal dose and changes in DCE-MRI parameters

Our patients were part of a large thermoradiotherapy clinical trial that tested effects of high versus low thermal dose in dogs with spontaneous soft tissue sarcomas (3). We reported that increased cumulative thermal dose was related to increased time to local failure. One potential mechanism underlying the improvement in local tumor control might be increased oxygenation, resulting from increased perfusion. However, we did not find an association between higher thermal dose and increased DCE-MRI parameters in this study (Table 4). It may be that patient-related parameters, such as the maturity of the vasculature or rates of tumor cell killing after the first thermoradiotherapy session, had more of an influence on perfusion changes than thermal dose itself. Additionally, we did not measure changes in oxygenation of these tumors, so we cannot conclude whether the changes in DCE-MRI parameters were associated directly with improvements in tumor oxygenation. Studies of this type are ongoing now in our group.

Our prior analysis also showed that duration of heating time, independent of thermal dose, was related to metastasis-free and overall survival. This recapitulates what we saw in the larger cohort of animals in this study (3). A reasonable assumption might be that duration of heating would be related to perfusion in some way. For example, the time required to reach the predetermined thermal dose would be shorter for more poorly perfused tumors. In this subset analysis, we found that duration of heating was still important for overall and metastasis-free survival, but it was not related to any of the DCE-MRI parameters. There was a correlation between duration of heating and tumor grade. Higher-grade tumors tended to take longer to adequately heat. This may have to do with a greater propensity for preexisting necrosis in high-grade tumors. Such tumors may develop power-limiting hotspots in necrotic areas, which could lead to the need to prolong heating times to get the rest of the tumor exposed to the prescribed thermal dose.

Using the same animals in this study, we recently reported that low pHe is associated with increased likelihood for tumor metastasis and shortened overall survival (14). The acidic environment within tumors is thought to exist because of metabolic aberrations leading to propensity for anaerobic metabolism (e.g., the Warburg effect) and/or induction of anaerobic metabolism as a result of hypoxia (e.g., the Pasteur effect). However, the degree of acidosis will also be influenced by how efficiently the lactate is removed from the tissue by perfusion. In this study, there was no relationship between DCE-MRI parameters obtained before treatment and pH, but an increase in washout was associated with an increase in pH. This is consistent with washout being indicative of a more efficient vascular system for waste removal. The inverse relationship between pHi and washout is more difficult to explain. Generally, pHi is tightly regulated by a variety of proton pumps that move lactate and hydrogen ions out of the cell to maintain a neutral pHi (32). It is difficult to reconcile how pHi could have any influence on changes in DCE-MRI parameters after hyperthermia treatment. This may be a spurious observation.

DCE-MRI analysis methods

There are two main models that have been used to derive physiologically based parameters from dynamic images. The first is a two-compartment model that includes the transfer coefficient between the intravascular and extravascular compartments (K^{trans}), the extracellular volume fraction, and

Table 3. Summary of univariable analysis showing the relationship between tumor volume and tumor grade with the significant perfusion/permeability estimators obtained with Gd-DTPA DCE-MRI

	Tumor volume		Tumor grade	
	Spearman	*P*	Exact rank sum test	*t* test
Pre				
AUC60	-0.239	0.155	0.256	0.3
AUC90	-0.241	0.151	0.242	0.294
AUCt-max	-0.208	0.216	0.124	0.182
Washin	-0.175	0.3	0.756	0.787
Washout	-0.293	0.079	0.141	0.189
Post				
AUC60	**-0.500**	**0.041**	0.506	0.379
AUC90	**-0.515**	**0.035**	0.646	0.346
AUCt-max	**-0.610**	**0.009**	**0.009**	**0.008**
Washin	**-0.534**	**0.027**	**0.234**	**0.039**
Washout	**-0.586**	**0.014**	0.328	0.189
HT (min)	0.244	0.146	**0.033**	0.104

NOTE: Summary of univariable analysis showing the relationship between tumor volume and tumor grade with the significant perfusion/permeability estimators obtained with Gd-DTPA DCE-MRI. All of the post-MRI image parameters were found to correlate with tumor volume. AUCt-max and washin correlated with tumor grade. Therefore, it is not possible to determine whether these parameters are independent predictors of outcome.

Table 4. Summary analysis showing the relationship between the MRI parameters measured to pH parameters

	pHi-Pre		pHi@24 h-pHi-Pre		pHe-Pre		pHe@24 h-pHe-Pre	
	Spearman	***P***	**Spearman**	***P***	**Spearman**	***P***	**Spearman**	***P***
Pre								
AUC60	0.034	0.868	0.169	0.563	0.023	0.912	0.02	0.93
AUC90	0.046	0.818	0.143	0.626	0.034	0.871	0.01	0.966
AUCt-max	-0.163	0.417	0.037	0.899	0.099	0.63	0.098	0.665
Washin	0.006	0.976	0.174	0.553	0.032	0.877	0.132	0.56
Washout	0.027	0.894	-0.486	0.078	0.149	0.467	-0.014	0.95
Post								
AUC60	-0.118	0.676	-0.036	0.916	0.256	0.358	0.086	0.761
AUC90	-0.125	0.657	0.036	0.916	0.256	0.358	0.125	0.657
AUCt-max	-0.236	0.398	0.036	0.916	0.225	0.42	0.254	0.362
Washin	-0.236	0.398	0.173	0.612	0.32	0.245	0.293	0.29
Washout	**-0.643**	**0.01**	0.182	0.593	-0.288	0.298	**0.736**	**0.002**
HT (min)	0.066	0.744	0.077	0.794	-0.204	0.317	-0.213	0.342

NOTE: Summary analysis showing the relationship between the MRI parameters measured to pH parameters. Only the difference between pHe pretherapy and posttherapy was found to correlate with post-washout values. Bold and shaded cells were significant and bolded image parameters were the ones significant in predicting outcome as shown in Table 1.

vascular volume fraction (33, 34). The second model is an empirical fit of the signal enhancement data of a pixel or region of interest. An AUC can be calculated with this empirical fit. AUC calculations and the fitted values of the empirical equation can then be used to evaluate the dynamic data and referenced to normal tissue, such as muscle (17, 29, 35–38). This second technique has the advantage of not requiring an arterial input function (arterial concentration-time curve of the contrast agent) for analysis.

All of these methods attempt to ascertain the meaning of the dynamic signal from DCE-MRI into physiologically tangible properties (i.e., tumor perfusion and vascular permeability). Several prior reports have shown correlations between DCE-MRI parameters and treatment outcome (27, 29, 31, 39–41).

In this study, we used the second method, fitting the signal enhancement curve to an empirical equation. From this analysis, several DCE-MRI parameters were associated with treatment outcome in this study. In all cases, parameters that were associated with better overall perfusion indicated a better outcome. Being able to predict overall treatment outcome before, or shortly after treatment is initiated, potentially allows for treatment modification, which may improve overall efficacy.

Limitations of the posttreatment data

Although the protocol called for scans to be taken before and 24 hours after the first hyperthermia treatment, only 17 of the original 37 animals actually had data at this second time point. There were multiple reasons for lack of data, but the two main ones related to lack of good data fits on the second session or scheduling conflicts. The scans were obtained on a human scanner and there were times when we were unable to schedule the canine patients for the second scan. We might have been able to avoid the poor data fitting on the second scan had we been able to analyze the results immediately after the scan was done. Unfortunately, this was not possible at the time that these studies were done. In fact, we did not know about the problem until years later when the data were post-analyzed. We have encountered similar problems previously in human (18) studies. This points to the need for more rapid evaluation of study-related parameters so that additional measurements could be made, thereby improving the data acquisition for studies that require multiple time points.

Canine sarcomas as models for human cancer

The canine sarcoma is an ideal model for human solid tumors in many respects. These advantages have been reviewed in detail but are briefly summarized here. The natural history of canine sarcomas is very similar to that of humans (42). They are locally invasive and a proportion of them metastasize, making the achievement of local control challenging. For the purposes of hyperthermia studies, they are of the same size range as human tumors, making them amenable to heating, using the same heating technologies that are used in humans. There are many advantages of the canine tumor model in general. The patients are outbred and they are typically older and therefore have concomitant diseases like human patients do. They are immune competent, yet their tumors are only weakly antigenic, similar to humans (42). We have used this model extensively over the last 25 years.

Conclusion

Although the number of tumors imaged was limited, the results of this study suggest that DCE-MRI perfusion parameters are associated with various indicators of prognosis. Because delivery of nutrients (oxygen) and removal of waste (lactate) are dependent on perfusion, imbalances in delivery of nutrients and waste removal may contribute to aggressiveness of soft tissue sarcomas.

Disclosure of Potential Conflicts of Interest

No potential conflicts of interest were disclosed.

References

1. Datta NR, Bose AK, Kapoor HK, Gupta S. Head and neck cancers: results of thermoradiotherapy versus radiotherapy. Int J Hyperthermia 1990;6:479–86.
2. Overgaard J, Gonzalez Gonzalez D, Hulshof MC, et al. Randomised trial of hyperthermia as adjuvant to radiotherapy for recurrent or metastatic malignant melanoma. European Society for Hyperthermic Oncology. Lancet 1995;345:540–3.
3. Thrall DE, LaRue SM, Yu D, et al. Thermal dose is related to duration of local control in canine sarcomas treated with thermoradiotherapy. Clin Cancer Res 2005;11:5206–14.
4. Valdagni R, Amichetti M. Report of long-term follow-up in a randomized trial comparing radiation therapy and radiation therapy plus hyperthermia to metastatic lymph nodes in stage IV head and neck patients. Int J Radiat Oncol Biol Phys 1994;28:163–9.
5. van der Zee J, Gonzalez Gonzalez D, van Rhoon GC, van Dijk JD, van Putten WL, Hart AA. Comparison of radiotherapy alone with radiotherapy plus hyperthermia in locally advanced pelvic tumours: a prospective, randomised, multicentre trial. Dutch Deep Hyperthermia Group. Lancet 2000;355:1119–25.
6. Jones EL, Oleson JR, Prosnitz LR, et al. Randomized trial of hyperthermia and radiation for superficial tumors. J Clin Oncol 2005;23:3079–85.
7. Song CW. Effect of local hyperthermia on blood flow and microenvironment: a review. Cancer Res 1984; 44:4721–30s.
8. Vujaskovic Z, Song CW. Physiological mechanisms underlying heat-induced radiosensitization. Int J Hyperthermia 2004;20:163–74.
9. Vujaskovic Z, Poulson JM, Gaskin AA, et al. Temperature-dependent changes in physiologic parameters of spontaneous canine soft tissue sarcomas after combined radiotherapy and hyperthermia treatment. Int J Radiat Oncol Biol Phys 2000;46:179–85.
10. Thrall DE, Larue SM, Pruitt AF, Case B, Dewhirst MW. Changes in tumour oxygenation during fractionated hyperthermia and radiation therapy in spontaneous canine sarcomas. Int J Hyperthermia 2006;22: 365–73.
11. Milligan AJ, Panjehpour M. Canine normal and tumor tissue estimated blood flow during fractionated hyperthermia. Int J Radiat Oncol Biol Phys 1985;11: 1679–84.
12. Brizel DM, Scully SP, Harrelson JM, et al. Radiation therapy and hyperthermia improve the oxygenation of human soft tissue sarcomas. Cancer Res 1996;56: 5347–50.
13. Jones EL, Prosnitz LR, Dewhirst MW, et al. Thermochemoradiotherapy improves oxygenation in locally advanced breast cancer. Clin Cancer Res 2004;10: 4287–93.
14. Lora-Michiels M, Yu D, Sanders L, et al. Extracellular pH and P-31 magnetic resonance spectroscopic variables are related to outcome in canine soft tissue sarcomas treated with thermoradiotherapy. Clin Cancer Res 2006;12:5733–40.
15. Bostock DE, Dye MT. Prognosis after surgical excision of canine fibrous connective tissue sarcomas. Vet Pathol 1980;17:581–8.
16. Belfi CA, Paul CR, Shan S, Ngo FQ. Comparison of the effects of hydralazine on tumor and normal tissue blood perfusion by MRI. Int J Radiat Oncol Biol Phys 1994;29:473–9.
17. Evelhoch JL. Key factors in the acquisition of contrast kinetic data for oncology. J Magn Reson Imaging 1999;10:254–9.
18. Dewhirst MW, Poulson JM, Yu D, et al. Relation between pO_2, ^{31}P magnetic resonance spectroscopy parameters and treatment outcome in patients with high-grade soft tissue sarcomas treated with thermoradiotherapy. Int J Radiat Oncol Biol Phys 2005;61: 480–91.
19. Dewhirst MW, Viglianti BL, Lora-Michiels M, Hanson M, Hoopes PJ. Basic principles of thermal dosimetry and thermal thresholds for tissue damage from hyperthermia. Int J Hyperthermia 2003;19:267–94.
20. Secomb TW, Hsu R, Braun RD, Ross JR, Gross JF, Dewhirst MW. Theoretical simulation of oxygen transport to tumors by three-dimensional networks of microvessels. Adv Exp Med Biol 1998;454:629–34.
21. Secomb TW, Hsu R, Dewhirst MW, Klitzman B, Gross JF. Analysis of oxygen transport to tumor tissue by microvascular networks. Int J Radiat Oncol Biol Phys 1993;25:481–9.
22. Secomb TW, Hsu R, Ong ET, Gross JF, Dewhirst MW. Analysis of the effects of oxygen supply and demand on hypoxic fraction in tumors. Acta Oncol 1995; 34:313–6.
23. SecombTW, Hsu R, Park EY, Dewhirst MW. Green's function methods for analysis of oxygen delivery to tissue by microvascular networks. Ann Biomed Eng 2004;32:1519–29.
24. Jain RK. Physiological barriers to delivery of monoclonal antibodies and other macromolecules in tumors. Cancer Res 1990;50:814–9s.
25. Jain RK. Haemodynamic and transport barriers to the treatment of solid tumours. Int J Radiat Biol 1991; 60:85–100.
26. Semenza GL. Targeting HIF-1 for cancer therapy. Nat Rev Cancer 2003;3:721–32.
27. Mayr NA, Yuh WT, Arnholt JC, et al. Pixel analysis of MR perfusion imaging in predicting radiation therapy outcome in cervical cancer. J Magn Reson Imaging 2000;12:1027–33.
28. Mayr NA, Yuh WT, Magnotta VA, et al. Tumor perfusion studies using fast magnetic resonance imaging technique in advanced cervical cancer: a new noninvasive predictive assay. Int J Radiat Oncol Biol Phys 1996;36:623–33.
29. Hoskin PJ, Saunders MI, Goodchild K, Powell ME, Taylor NJ, Baddeley H. Dynamic contrast enhanced magnetic resonance scanning as a predictor of response to accelerated radiotherapy for advanced head and neck cancer. The British journal of radiology 1999; 72:1093–8.
30. Pickles MD, Lowry M, Manton DJ, Gibbs P, Turnbull LW. Role of dynamic contrast enhanced MRI in monitoring early response of locally advanced breast cancer to neoadjuvant chemotherapy. Breast Cancer Res Treat 2005;91:1–10.
31. Dunst J, Ahrens S, Paulussen M, Burdach S, Jurgens H. Prognostic impact of tumor perfusion in MR-imaging studies in Ewing tumors. Strahlenther Onkol 2001;177:153–9.
32. Madshus IH. Regulation of intracellular pH in eukaryotic cells. Biochem J 1988;250:1–8.
33. Tofts PS, Brix G, Buckley DL, et al. Estimating kinetic parameters from dynamic contrast-enhanced T(1)-weighted MRI of a diffusable tracer: standardized quantities and symbols. J Magn Reson Imaging 1999;10:223–32.
34. Leach MO, Brindle KM, Evelhoch JL, et al. The assessment of antiangiogenic and antivascular therapies in early-stage clinical trials using magnetic resonance imaging: issues and recommendations. Br J Cancer 2005;92:1599–610.
35. Lyng H, Vorren AO, Sundfor K, et al. Assessment of tumor oxygenation in human cervical carcinoma by use of dynamic Gd-DTPA-enhanced MR imaging. J Magn Reson Imaging 2001;14:750–6.
36. Tuncbilek N, Karakas HM, Okten OO. Dynamic contrast enhanced MRI in the differential diagnosis of soft tissue tumors. Eur J Radiol 2005;53:500–5.
37. Siegmann KC, Muller-Schimpfle M, Schick F, et al. MR imaging-detected breast lesions: histopathologic correlation of lesion characteristics and signal intensity data. AJR Am J Roentgenol 2002;178:1403–9.
38. Hawighorst H, Knapstein PG, Knopp MV, Vaupel P, van Kaick G. Cervical carcinoma: standard and pharmacokinetic analysis of time-intensity curves for assessment of tumor angiogenesis and patient survival. Magma 1999;8:55–62.
39. Wong ET, Jackson EF, Hess KR, et al. Correlation between dynamic MRI and outcome in patients with malignant gliomas. Neurology 1998;50:777–81.
40. Mayr NA, Taoka T, Yuh WT, et al. Magnetic resonance imaging in the assessment of radiation response in cervical cancer: regarding Hatano K et al. IJROBP 1999; 45:399-344. Int J Radiat Oncol Biol Phys 2000;48:910–2.
41. Postema S, Pattynama PM, van Rijswijk CS, Trimbos JB. Cervical carcinoma: can dynamic contrast-enhanced MR imaging help predict tumor aggressiveness? Radiology 1999;210:217–20.
42. Dewhirst MW, Thrall D, MacEwen EG. Spontaneous pet animal cancers. In: Teicher B, editor. Tumor models in cancer research. Totowa (NJ): Humana Press; 2002. p. 565–90.